Available online at www.sciencedirect.com
SCIENCE DIRECT®
Continental Shelf Research 25 (2005) 1825–1835
CONTINENTAL SHELF RESEARCH
www.elsevier.com/locate/csr

Dimethylsulfide photolysis rates and apparent quantum yields in Bering Sea seawater

Clara J. Deal[a,*], David J. Kieber[b], Dierdre A. Toole[c], Knut Stamnes[d], Shigan Jiang[e], Naoaki Uzuka[a]

[a]*International Arctic Research Center, University of Alaska Fairbanks, P.O. Box 757335, Fairbanks, AK 99775-7335, USA*
[b]*Chemistry Department, College of Environmental Science and Forestry, State University of New York, One Forestry Drive, Syracuse, NY 13210, USA*
[c]*Department of Marine Chemistry and Geochemistry, Woods Hole Oceanographic Institution, Woods Hole, MA 02543-1050, USA*
[d]*Department of Physics and Engineering Physics, Stevens Institute of Technology, Castle Point on Hudson, Hoboken, NJ 07030, USA*
[e]*Atmospheric Sciences Research Center, State University of New York, 251 Fuller Road, Albany, NY 12203, USA*

Received 15 July 2004; received in revised form 23 March 2005; accepted 13 June 2005
Available online 22 August 2005

Abstract

Wavelength dependence and modeled rates of dimethylsulfide (DMS) photolysis were determined in seawater from two Bering Sea stations in August 2001. Monochromatic irradiations were employed to determine wavelength-dependent apparent quantum yields ($AQY_{DMS}(\lambda)$). $AQY_{DMS}(\lambda)$ scaled to 1 nM DMS decreased exponentially with increasing wavelength, ranging from 3.8×10^{-6} at 290 nm to 4.7×10^{-8} at 400 nm. No appreciable loss of DMS was observed in dark controls or at visible wavelengths ($\lambda \geqslant 400$ nm). DMS photolysis rates were calculated using experimentally determined $AQY_{DMS}(\lambda)$, spectral chromophoric dissolved organic matter (CDOM) absorption coefficients ($a_{CDOM}(\lambda)$), and simulated spectral scalar irradiance derived from a coupled atmosphere–ocean radiative transfer model. DMS photolysis rate estimates indicated that ~72–78% of DMS photolysis was observed in the UVA (320–400 nm) region, with a maximum response near 330–340 nm. Results from monochromatic and polychromatic irradiations agreed well, with the latter showing ~71% DMS photolysis in the UVA and ~29% attributed to UVB (280–320 nm). This supports the assertion that DMS photolysis is primarily driven by UV radiation. Turnover rate constants for DMS photolysis and sea-to-air fluxes in the upper 20 m of the water column were comparable, ranging between 0.02 and 0.11 d^{-1} and 0.13 and 0.26 d^{-1}, respectively, in the late summer non-bloom phase of the Bering Sea.

Keywords: Photochemistry; Biogeochemical cycles; Dimethylsulfide; Photolysis; Chromophoric dissolved organic matter; Chemical Oceanography; USA; Alaska; Bering Sea

*Corresponding author. Tel.: +1 907 474 1875; fax: +1 907 474 2643.
E-mail address: deal@iarc.uaf.edu (C.J. Deal).

0278-4343/$ - see front matter © 2005 Elsevier Ltd. All rights reserved.
doi:10.1016/j.csr.2005.06.006

1. Introduction

The southeastern Bering Sea is one of the world's most productive marine ecosystems with an abundance of dimethylsulfoniopropionate (DMSP)-producing algae. Marine algae that thrive in the Bering Sea include ice algae, the two Prymnesiophyte taxa: *Phaeocystis* spp., *Emiliania huxleyi* (blooms recorded in the Bering Sea since 1997) and diatoms (Matrai and Vernet, 1997), all strong producers of DMSP (Barnard et al., 1984; Keller et al., 1989a, b; Levasseur et al., 1994: Matrai et al., 1995), the biological precursor to dimethylsulfide (DMS). Considering the magnitude and duration of blooms of these DMSP producing species and the strong feedbacks that exist in the polar climate system (e.g., ice-albedo and cloud radiation effects), the Bering Sea is an opportune setting to investigate possible climatic feedbacks between DMS flux and climate. However, the strength and sign of any feedback remains unknown largely due to our limited knowledge of the spatiotemporal variability of the biogeochemical cycling of DMS in the upper ocean. In the past three decades, major changes in southeastern Bering Sea ecosystems have occurred (Hunt et al., 2002) but the mechanisms linking these changes and climate forcing are unclear. Before we can evaluate the contributing role of DMS, we need a much better understanding of its biogeochemical cycling at northern high latitudes, namely the significance of the various oceanic sources and sinks.

The biogeochemical cycling of DMS in seawater involves a complex marine food web interacting within a dynamic physical and chemical environment. The production of DMS in the upper ocean results from grazing, direct exudation, senescence, viral or bacterial attack, physical or chemical stress (e.g., Wakeham and Dacey, 1989; Wolfe and Steinke, 1996; Nguyen et al., 1988; Hill et al., 1998; Sunda et al., 2002), and heterotrophic bacterial consumption of dissolved DMSP (DMSPd) to produce DMS. These sources of DMS are balanced by three DMS removal processes: bacterial consumption, photolysis, and sea-to-air ventilation (Brimblecombe and Shooter, 1986; Kiene and Bates, 1990; Bates et al., 1994; Kieber et al., 1996; Slezak et al., 2001; Toole et al., 2003, 2004; Bouillon and Miller, 2004). Photolysis of DMS is an important loss process in the euphotic zone (Kieber et al., 1996; Brugger et al., 1998; Hatton, 2002; Toole et al., 2003), periodically controlling the loss of DMS in the upper mixed layer (Kieber et al., 1996; Toole et al., 2004).

A critical component for computing DMS photolysis rates is the spectral apparent quantum yield ($AQY_{DMS}(\lambda)$). $AQY_{DMS}(\lambda)$ have been measured recently in oligotrophic Sargasso Sea seawater (Toole et al., 2003) and in an in situ iron-induced bloom in the Northeastern Subarctic Pacific Ocean (Bouillon and Miller, 2004). Evaluating the variability in $AQY_{DMS}(\lambda)$ for DMS photolysis is needed to extrapolate $AQY_{DMS}(\lambda)$ values beyond measurement sites, and to understand this DMS loss process and assess its significance in the oceanic DMS biogeochemical cycle. An important question explored in this work, and recently by Toole et al. (2003) and Bouillon and Miller (2004), is what are the wavelength-resolved apparent quantum yields for the photolysis of DMS in seawater? Furthermore, to what extent are $AQY_{DMS}(\lambda)$ similar in contrasting water types? The answers to these questions are critical for modeling DMS photolysis and improving our understanding of how DMS photochemistry affects the net production of DMS in seawater. To this end we present $AQY_{DMS}(\lambda)$ from the biologically productive Bering Sea during late-summer, stratified, productive upper ocean conditions.

2. Experimental methods

2.1. Sample collection

The Bering Sea is a semi-enclosed, high-latitude sea, divided almost equally between a deep basin and continental shelves characterized by a broad shelf in the east (>500 km) and a narrow shelf in the west (<100 km). The southeastern shelf is differentiated into three regions, or domains (coastal, middle and outer), by changes in mixing energy and topographic features (Coachman, 1986). During the fall and winter, the middle

domain of the water column (50–100 m) is generally homogeneous. In the spring, increased buoyancy in the surface layer results in a two-layered vertically stratified water column, setting up a pronounced thermocline with a wind-mixed surface layer (15–40 m) that persists throughout the summer. The outer shelf domain (100–200 m) has an intermediate layer separating the wind-mixed surface layer and a tidally mixed bottom layer that persists throughout the year.

Seawater samples were collected on the JAMSTEC R/V *Mirai* cruise, Leg 2 MR01-K04, from the outer shelf (Station 1, 166° 00.0W, 54° 59.9N) and middle shelf (Station 7, 166° 00.0W, 57° 59.9N) of the southeastern Bering Sea on August 28 and 30, 2001, respectively (Fig. 1), at 5 m employing a CTD rosette sampler with 12 L Niskin bottles. Mixed layer depths were 40 and 20 m for stations 1 and 7, respectively. At the time of sample collection the temperature, salinity, nitrate (at 5 m), and wind speed were 9.5 °C, 32.4 ppt, 4.7 μM, and 6.6 m s^{-1} for station 1, and 9.3 °C, 31.5 ppt, <1 μM, and 9.7 m s^{-1} for station 7 (JAMSTEC Preliminary Cruise Report, 2001). No obvious coccolithophore bloom was observed at either station, chlorophyll *a* concentrations were 0.8–1.2 mg m^{-3}, and HPLC pigment data indicated that prymnesiophytes and diatoms predominated at both sites (Hiroshi Hattori, pers. comm.).

Sample handling and collection procedures are described in detail by Toole et al. (2003). Briefly, seawater samples were gravity filtered directly from Niskin sampling bottles through a 0.2 μm Whatman POLYCAP filter attached using silicon tubing. The filtered seawater was kept at 4 °C in pre-cleaned glass Qorpak bottles wrapped in aluminum foil for 8 weeks before analysis. Results of a recent storage study (Deal et al., unpublished data) showed that this cleaning and preservation procedure ensured sample integrity through at least 8 weeks of storage as determined by absorbance spectroscopy (i.e., no change in the sample UV-Vis absorbance spectrum was observed).

2.2. Laboratory photochemical studies

DMS concentrations, chromophoric dissolved organic matter (CDOM) absorption coefficient spectra ($a_{CDOM}(\lambda)$), and photon fluxes were

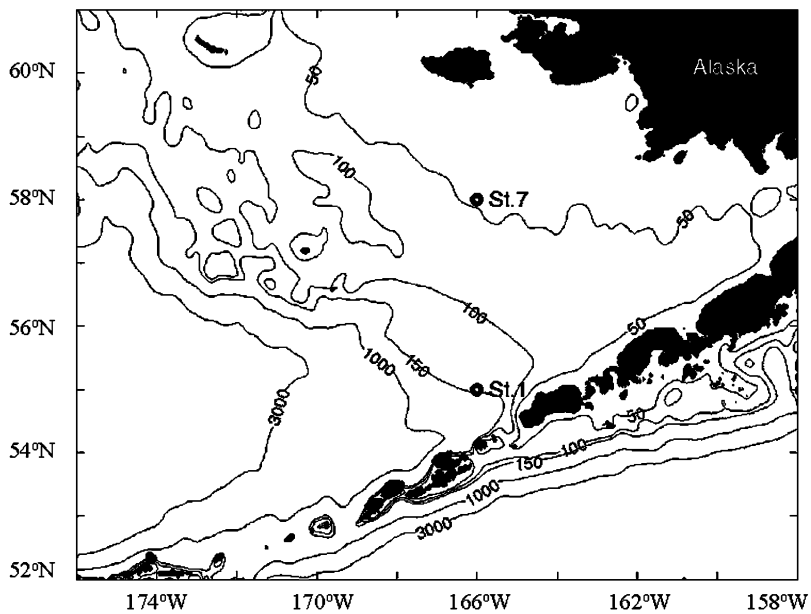

Fig. 1. Sampling locations for Station 1 (middle domain, MLD = 40 m, depth = 55 m) and Station 7 (outer domain, MLD = 20 m, depth = 135 m).

determined employing published procedures (Toole et al., 2003). DMS concentrations were measured using a Shimadzu GC-14A gas chromatograph equipped with a flame photometric detector and a Chromosil 330 column (Supelco). The analytical precision was in most cases $\pm 2\%$ at 20 nM DMS, and in all cases never more than $\pm 3\%$. CDOM absorption coefficient spectra were determined using a Hewlett Packard 8453 UV-VIS photodiode array spectrophotometer equipped with a 5 cm quartz microliter flow cell.

The wavelength dependence for DMS photolysis in the Bering Sea was determined following the procedure of Kieber et al. (1996) further detailed in Toole et al. (2003). Briefly, an illumination system equipped with a 1000 W xenon arc lamp and a Spectral Energy GM 252 high-intensity grating monochromator was used to measure DMS photolysis rates at 10 nm wavelength bandwidths between 290 and 400 nm. All seawater samples were irradiated at 21 °C in a continually stirred 1 cm-pathlength quartz cell containing 3.5 mL sample with ~20 nM DMS added and no headspace. Percentage loss (2% to 20%) and rate constants for DMS photolysis were calculated from DMS concentrations before and after irradiation. Additionally, comparisons of CDOM absorption coefficients before and after irradiation revealed no measurable change indicating that CDOM absorption coefficients were constant over the time course of irradiation. A borosilicate longpass filter was placed in front of the cell holder for irradiations at wavelengths greater than 310 nm to remove second-order diffraction. The light flux was determined by nitrite actinometry (Jankowski et al., 1999, 2000). Dark controls were examined by incubating samples in the 1 cm cell in the cell holder and blocking the incoming light for a period of time corresponding to the longest irradiation at each wavelength.

Incubations were also conducted under natural light on the rooftop in Syracuse, NY for comparison to laboratory irradiations. Station 1 seawater was placed in quartz tubes (Kieber et al., 1997) and incubated in a circulating water bath for 6 h with different spectral treatments: (1) quartz tubes (full sunlight), (2) aluminum foil-wrapped quartz tubes (dark), (3) Mylar-D wrapped quartz tubes, transmitting 60–80% of UVA and very little UVB, and (4) UF3 Plexiglas-enclosed quartz tubes, attenuating essentially all UVA and UVB with 92% of visible light transmitted. For transmission spectra of Mylar D and UF3 Plexiglas see Miller (2000).

2.3. Apparent quantum yields

The photochemical quantum yield is the probability that an absorbed photon will bring about a reaction. Since the photochemical reaction rate is the product of the quantum yield and the probability that an incident photon will be absorbed, the photochemical quantum yield can be expressed as:

$$AQY_{\mathrm{DMS}}(\lambda) = \frac{(\mathrm{d}[\mathrm{DMS}]_{\lambda}/\mathrm{d}t)\,V}{E_{\lambda}(\lambda)(1-10^{-A_{\lambda}})}, \quad (1)$$

where $AQY_{\mathrm{DMS}}(\lambda)$ is the wavelength-dependent apparent quantum yield for DMS photolysis, $\mathrm{d}[\mathrm{DMS}]_{\lambda}/\mathrm{d}t$ is the change in DMS concentration during an irradiation (i.e., the DMS photolysis rate), V is the cell volume (L), E_{λ} is photon flux (mol quanta min^{-1}) and A_{λ} is the CDOM absorbance with the fraction of incident flux absorbed by CDOM denoted as $(1-10^{-\mathrm{A}\lambda})$. Since photolysis of DMS follows pseudo-first-order kinetics (e.g. Kieber and Jiao 1995; Kieber et al. 1996; Brugger et al. 1998), the $\mathrm{AQY}_{\mathrm{DMS}}(\lambda)$ and therefore DMS photolysis rate term in Eq. (1) are directly proportional to the initial DMS concentration. Thus, the $\mathrm{AQY}_{\mathrm{DMS}}(\lambda)$ scaled to 2 nM DMS will be twice that at 1 nM DMS.

Since the chromophores involved in DMS photolysis are not known and DMS photolysis rates covary with CDOM absorbance (Kieber and Jiao 1995), the absorption of photons by CDOM was used as a proxy for reactant absorption in the quantum yield expression. The $\mathrm{AQY}_{\mathrm{DMS}}(\lambda)$ determined here is thus an estimated minimum because the light absorbing reactant(s) is most likely a subset of the total CDOM absorption. The term apparent quantum yield reflects our uncertainty in the chromophore(s) resulting in DMS photolysis. $\mathrm{AQY}_{\mathrm{DMS}}(\lambda)$ is also concentration (vide supra) and temperature dependent (Toole et al., 2003; Bouillon and Miller 2004). Here we present $\mathrm{AQY}_{\mathrm{DMS}}(\lambda)$ scaled to 1 nM DMS and 21 °C.

Modeled photolysis rates were calculated using $AQY_{DMS}(\lambda)$ corrected to the ambient Bering Sea temperature at 5 m (ca. 9 °C) using the relationship established by Toole et al. (2003).

2.4. Simulated UV scalar irradiance

Water column irradiance profiles were estimated from a radiative transfer model for the coupled atmosphere-ocean (CAO) system based on the discrete ordinate method (CAO-DISORT model). This model allows computation of radiative quantities (irradiance, radiance, scalar irradiance) at any height in the atmosphere or depth in the water column (Jin and Stamnes, 1994; Thomas and Stamnes, 1999). It was validated against measurements in the visible and UV spectral range (Thomas and Stamnes, 1999) and against Monte Carlo simulations (Gjerstad et al., 2003), and was found to provide accurate results for known inherent optical properties (IOP, input parameters). Although the model has been validated against UV measurements obtained in Antarctica, it has not been validated for the Bering Sea. Unfortunately, there are no underwater UV radiation measurements available from the two sampling events for model-data comparison.

For our Bering Sea study, water column inherent optical properties in the UV range, needed as input to the CAO-DISORT model, were estimated. The measured absorption coefficients of pure water $a_w(\lambda)$ from Pope and Fry (1997) were used, extrapolating below 380 nm based on data from Smith and Baker (1981). Phytoplankton absorption coefficients ($a_{ph}(\lambda)$) were estimated as the product of the specific absorption of chlorophyll ($a_{ph}*(\lambda)$) for polar *Phaeocystis* spp. obtained from Soo Hoo et al. (1987) and the observed concentrations of chlorophyll at stations 1 and 7. $a_{CDOM}(\lambda)$ measured at 5 m for both stations were used throughout the surface mixed layer, as the summer mixed layer in the southeastern Bering Sea is homogeneous due to frequent storms and high wind events. We did not measure the absorption coefficient for detrital particles ($a_d(\lambda)$) in the Bering Sea and thus do not consider $a_d(\lambda)$ in the model. As a result our simulated UV spectral irradiances may be biased high, but not significantly, as Nelson and Siegel (2002) suggest that detrital particles make only a small contribution to the total absorption of UV light in the ocean. Surface layer measurements of $a_{CDOM}(\lambda)$ and $a_d(\lambda)$ from 400 to 700 nm made by Sasaki et al. (2001) in the summer 1997 at 57°00.0 N, 166°00.0 W (1°N of station 1 and 2°S of station 7 in our study) lend credence to this assumption. They observed that at 400 nm, the relative contributions from $a_{CDOM}(\lambda)$ and $a_d(\lambda)$ were 84% and 5%, respectively. Their measurements of $a_d(400)$ were $<0.01\ m^{-1}$ at depths shallower than 15 m. Considering that the spectral shape of $a_d(\lambda)$ is similar to that of $a_{CDOM}(\lambda)$ (Nelson and Siegel, 2002), and that our measurements of $a_{CDOM}(400)$ were $>0.15\ m^{-1}$, our assumption that detrital particles make only a small contribution to the absorption of UV light is supported. The total absorption coefficient used to model UV scalar irradiance in the water column is thus the sum of the component absorption due to pure seawater, phytoplankton, and CDOM. The total scattering coefficient $b(\lambda)$ was estimated as a function of the measured chlorophyll concentration using a standard bio-optical algorithm (Morel, 1980; Gordon and Morel, 1983; Morel and Maritorena, 2001) and scattering by pure water (Morel, 1974). The Henyey-Greenstein phase function was adopted in the computations with an asymmetry factor of 0.90. We simulated spectral scalar irradiances for clear and overcast days (cloud extinction coefficients of 0.1 and 8, respectively) at both stations.

2.5. Turnover rate constants

Turnover rate constants, k_τ, were determined in the upper 20 m in order to evaluate the relative importance of atmospheric ventilation and photolysis as loss mechanisms for upper water column DMS. The turnover rate constant for atmospheric ventilation was calculated by dividing calculated DMS sea-to-air flux by the column-integrated DMS concentration between the sea surface and 20 m. Similarly the photochemical k_τ was calculated by dividing the modeled column-integrated photolysis rate by the column-integrated DMS concentration down to 20 m. $AQY_{DMS}(\lambda)$ used to calculate the modeled photolysis rates were scaled

to in situ DMS concentrations. The 0–20 m depth interval was selected for k_τ calculations since modeled estimates suggest that less than 1% of the UV light penetrated below 20 m at either station. The sea-to-air flux of DMS was estimated from the product of the DMS concentration at 5 m ($\mu mol\,m^{-3}$) measured on the JAMSTEC R/V *Mirai* cruise, Leg 2 MR01-K04 (Uzuka et al., 2001; JAMSTEC Preliminary Cruise Report, 2001, pp. 93–94) and an empirically derived transport velocity ($m\,d^{-1}$; Wanninkhof and McGillis, 1999), modeled as a function of seawater temperature, local wind speed and DMS gas diffusivities from Saltzman et al. (1993). The average wind speed for the sampling period was used. The calculations assumed that DMS concentrations and CDOM absorption coefficients were constant over the one day time period.

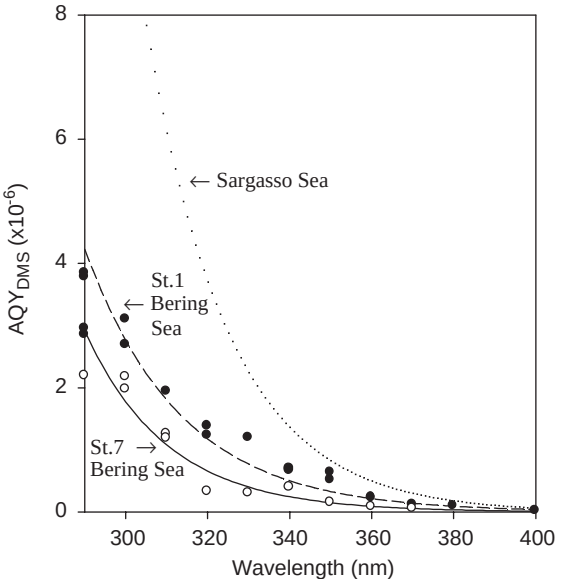

Fig. 2. Wavelength-dependent apparent quantum yields for DMS photolysis ($AQY_{DMS}(\lambda)$, mol DMS photolyzed/mol photons absorbed by CDOM) measured in the laboratory at 21 °C and scaled to 1 nM DMS. Station 1 (166 °00.0′W 54 °59.9′N, ●) is in the outer shelf and station 7 (166°00.0′W 57 °59.9′N, ○) is in the middle shelf of the southeastern Bering Sea. The solid (station 7, Bering Sea, 5 m), dashed (station 1, Bering Sea, 5 m) and dotted (Sargasso Sea, 15 m, nominally 85 km southeast of the island of Bermuda on July 19, 2001, from Toole et al., 2003) lines denote the best fit of the data obtained from non-linear regression analysis.

3. Results and discussion

3.1. Apparent quantum yields

$AQY_{DMS}(\lambda)$ from 290 to 380 nm decreased exponentially with increasing wavelength at stations 1 and 7 (Fig. 2), and were well described by exponential decay functions ($r^2 = 0.947$, station 1; $r^2 = 0.948$, station 7):

$$AQY_{DMS}(\text{station 1}) = [\text{DMS}]1.01\,e^{-0.0427x} \quad (2)$$

$$AQY_{DMS}(\text{station 7}) = [\text{DMS}]5.14e^{-0.0497x} \quad (3)$$

scaled to the DMS concentration ([DMS]). Dark losses of DMS attributed to diffusion through the Teflon-faced silicone septum in the 1 cm quartz cuvette were negligible, accounting for less than 3% DMS loss in 16 h. Spectral slopes (± se) for the $AQY_{DMS}(\lambda)$ in the Bering Sea samples at station 1 ($0.0427 \pm 0.0024\,nm^{-1}$) and station 7 ($0.0497 \pm 0.0039\,nm^{-1}$) were remarkably similar to the spectral slope obtained from the summertime mixed-layer (15 m) Sargasso Sea sample ($0.0499\,nm^{-1}$, Toole et al., 2003), even though the Sargasso Sea is highly oligotrophic while the Bering Sea is biologically productive in the summer. This suggests that similar chromophores/mechanism(s) may have been responsible for the observed DMS loss in these two divergent oceanographic waters. However, while the slopes were similar, $AQY_{DMS}(\lambda)$ from the Bering Sea were significantly lower than those reported for the Sargasso Sea at all wavelengths examined (Fig. 2). For example, at the wavelength of peak DMS photolysis response in sunlight (ca. 330 nm; vide infra), the $AQY_{DMS}(\lambda)$ for the Sargasso Sea sample is approximately a factor of three larger than the corresponding $AQY_{DMS}(330)$ in the Bering Sea at station 1 (2.25×10^{-6} vs. 0.77×10^{-6}) and nearly an order of magnitude greater than at station 7 (0.39×10^{-6}). Most of the observed difference is thought to arise from the relative proportion of photosensitizing CDOM to the total amount of CDOM present and the higher spectral absorbance of the Bering Sea samples (Fig. 3) compared to the Sargasso Sea sample. The

differences in $AQY_{DMS}(\lambda)$ are even more striking when considering that nitrate affects quantum yields and rate constants for DMS photolysis (Bouillon and Miller, 2004; Toole et al., 2004). Bouillon and Miller (2004) noted a strong positive correlation between $AQY_{DMS}(330)$ and nitrate concentrations in the northeastern Subarctic Pacific Ocean. The $AQY_{DMS}(330)$ values for the Bering Sea seawater samples (0.77×10^{-6} for station 1 and 0.39×10^{-6} for station 7) at 4.5 and 1 μM nitrate, respectively, approximate the linear regression line shown in Fig. 3 of Bouillon and Miller (2004) (Fig. 4). This is not unexpected given that the Bering Sea is an extension of the Subarctic Pacific (Whitledge and Luchin, 1999). At the same time, nitrate concentrations in the Bering Sea seawater samples are substantially higher than those in the surface mixed layer of the Sargasso Sea seawater (nitrate < 0.1 μM), leading one to expect a priori that the $AQY_{DMS}(\lambda)$ in the Bering Sea samples would be higher than those in the Sargasso Sea. As this was not the case, we suggest that although $AQY_{DMS}(\lambda)$ is correlated to nitrate concentrations, nitrate is a relatively minor component accounting for the differences in the $AQY_{DMS}(\lambda)$ and that DOM is likely driving the photolysis of DMS in these waters. This was the case in Antarctic waters, where it was observed that chromophores other than nitrate were primarily responsible for the photolysis of DMS (Toole et al., 2004).

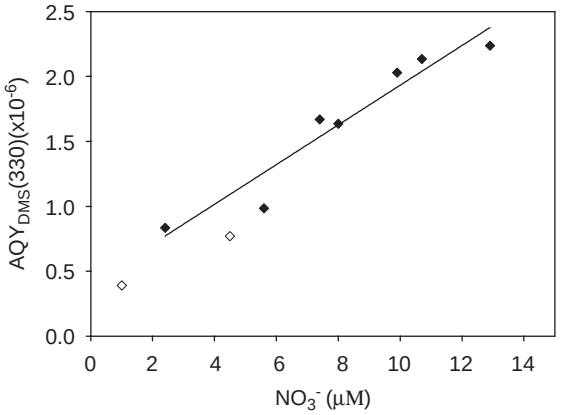

Fig. 4. Relationship between nitrate (NO_3^-) concentration and $AQY_{DMS}(330)$ (mol DMS photolyzed/mol photons absorbed by CDOM) for DMS photolysis near Ocean Station Papa (50°12′N, 144°45′W) in the northeastern Subarctic Pacific Ocean in July, 2002 (◆, see Bouillon and Miller, 2004) and $AQY_{DMS}(330)$ for the Bering Sea stations (◇). Line denotes best fit of the Bouillon and Miller (2004) data obtained from linear regression analysis. All AQY are scaled to 1 nM DMS.

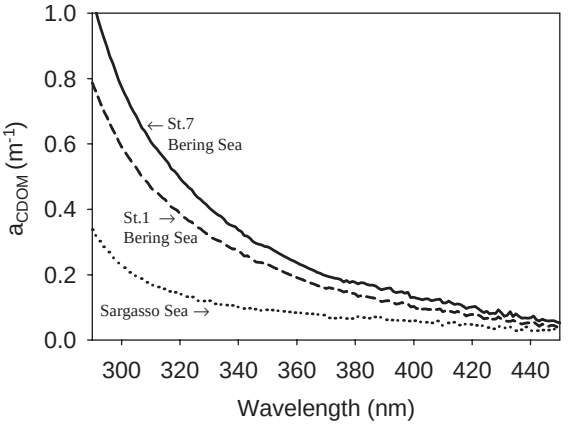

Fig. 3. CDOM absorption coefficient spectra for station 1 (dashed) and station 7 (solid) in the southeastern Bering Sea. The 15 m Sargasso Sea CDOM absorption coefficient spectrum (dotted) is also shown for comparison (Toole et al., 2003). Data collected from the diode array were used for wavelengths 290–450 nm except for smoothing between 350 and 370 nm, which was carried out using a standard CDOM exponential functional relationship (Green and Blough, 1994).

3.2. Spectral DMS photolysis rates

Calculated $AQY_{DMS}(\lambda)$ (Eqs. 2 and 3) were used in conjunction with estimated scalar irradiance data and CDOM absorbance data (Fig. 3) to derive spectrally resolved photolysis rates (Fig. 5). A CAO radiative transfer model was used to estimate the depth-dependent scalar irradiance at resolutions of 1 nm and 1 m depth, integrated between sunrise and sunset.

The spectrally resolved photolysis rate (PO) was determined at the sea surface (top 1 m) using the depth-integrated approach outlined in Toole et al. (2003):

$$PO = \int_t \int_z \int_\lambda AQY_{DMS}(\lambda) a_{CDOM}(\lambda) \times E_0(z, \lambda, t)\, dt\, dz\, d\lambda, \quad (4)$$

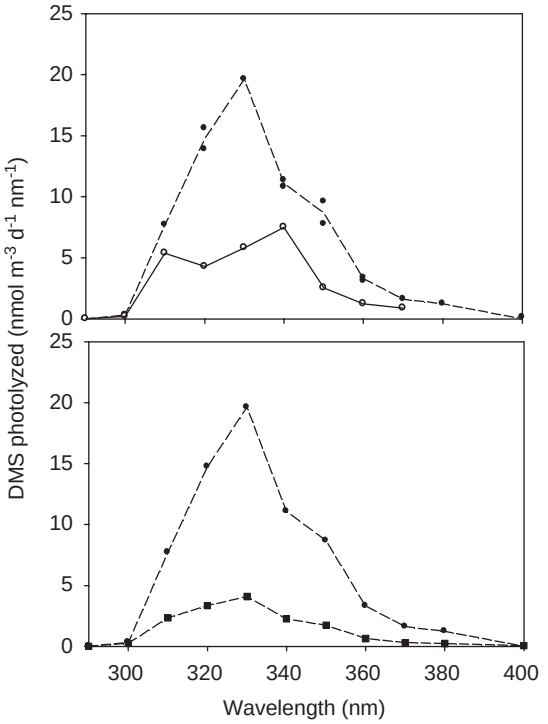

Fig. 5. DMS photolysis rates (i.e. product of $AQY_{DMS}(\lambda)$ scaled to 1 nM DMS, $a_{CDOM}(\lambda)$, and simulated scalar irradiance (λ)) plotted as a function of wavelength for the top 1 m of the water column at (above) stations 1 and 7 under clear sky conditions (● and ○, respectively) and (below) station 1 for clear (●) and overcast (■) conditions.

where $E_0(z, \lambda, t)$ is the wavelength, depth, and time-dependent spectral scalar irradiance (mol quanta m^{-2}). Wavelength-dependent photolysis rates were calculated for both stations using model-simulated clear and overcast sky conditions. In all cases, and for both stations, the maximum rate of photolysis was observed between 330 and 340 nm, with >70% of the total photolysis occurring in the UVA (Fig. 5).

Results from the rooftop incubation experiment were in agreement with wavelength dependencies observed in the monochromatic laboratory irradiation experiments. In the rooftop experiment, DMS loss was greatest in seawater incubated in quartz containers (full light) while no DMS loss was observed in seawater incubated under UV-attenuating UF3 Plexiglas (i.e. <6% DMS loss as observed in the dark control); the UF3 Plexiglas cutoff is 400 nm, attenuating essentially all the UV and transmitting 92% of the visible light. DMS loss in the Mylar-wrapped quartz tube (313 nm cutoff with 50% transmission at 320 nm and 60–80% transmission in the UVA) was slightly more than half that measured in the quartz containers. Differences between these treatments indicated that ~71% of DMS photolysis occurred in the UVA. Incubations under natural light support the laboratory irradiation experiments that show that DMS photolysis occurs at wavelengths in the UV spectral range. Our results are similar to those observed by other investigators (Toole et al., 2003; Toole et al., 2004) who showed that DMS photolysis occurs primarily in the UVA (61.2% and 79.6%, and ~65%, respectively).

3.3. Turnover rate constant comparison

Turnover rate constants calculated in the upper 20 m for stations 1 and 7 in the Bering Sea are listed in Table 1. The sea-to-air flux turnover rate constant (k_τ) for station 1 (0.13 d^{-1}) was lower than at station 7 (0.26 d^{-1}) owing to the lower average wind speed, 6.6 m s^{-2} compared to 9.7 m s^{-1}, respectively.

The photolysis turnover rate constant (k_τ) for station 7 (0.04 d^{-1}, clear sky) is lower than that for station 1 (0.10 d^{-1}, clear sky) due to the lower $AQY_{DMS}(\lambda)$ at station 7 and the higher 0–20 m column-integrated DMS concentration. Under overcast conditions, the k_τ for photolysis (0.02 d^{-1}, station 7; 0.03 d^{-1}, station 1) is substantially smaller by approximately a factor of three than the k_τ observed under clear sky conditions; and it is only a minor loss when compared to the k_τ for the sea-to-air flux. Calculations of the k_τ for photolysis under simulated clear and overcast conditions serve as

Table 1
Turnover rate constants for DMS photolysis and DMS sea-to-air flux calculated for stations 1 (August 28, 2001) and 7 (August 30, 2001) in the Bering Sea

Station	$K\tau_{sea-air}(d^{-1})$	$K\tau_{photo}$ clear(d^{-1})	$K\tau_{photo}$ overcast (d^{-1})
1	0.13	0.11	0.03
7	0.26	0.04	0.02

boundary conditions for this time of year. As can be expected, the importance of DMS photolysis decreases when cloud cover increases and the importance of DMS ventilation is less when winds are low. Considering that overcast conditions predominate over clear skies and that the average summer wind speed is 5.8 m s^{-1} (National Climate Data Center, 2002), the DMS sea-to-air flux is likely a more important loss process than photolysis in the southeastern Bering Sea during the summer.

Comparison studies of DMS loss processes and related factors beyond DMS photolysis and ventilation are needed, especially at high latitudes. In this study, we did not investigate bacterial degradation of DMS, which presumably occurs throughout the upper water column. Studies point to a leading role of bacteria in both the production and loss of DMS (Bates et al., 1987; Kiene and Service, 1991). Without determinations of the rate of bacterial degradation of DMS, it is not possible to ascertain how important photochemical loss is as a DMS sink in the water column relative to its biological removal. Results from a recent Antarctic cruise in the vicinity of the Ross Sea during the austral spring indicate, however, that biological consumption rates may be quite low under non-bloom conditions in polar climates (Toole et al. 2004). Vertical mixing is another factor that needs to be investigated further. The depth of the mixed layer and speed of mixing determines the average light exposure of a parcel of water and thus its potential photolysis rate (Huot et al. 2000; Neale and Kieber 2000; Preiswerk and Najjar 2000; Miller et al. 2002). Changing mixed layer dynamics may also result in a change in the relative importance of DMS loss pathways (including DMS photolysis) and in net DMS production. High resolution, Lagrangian sampling campaigns in tandem with modeling of the DMS oceanic cycle, including mixed layer dynamics, are needed to study how the various loss and production pathways interact to determine DMS seawater concentrations.

4. Conclusions

Extrapolating spectral apparent quantum yields for dimethylsulfide (DMS) photolysis ($AQY_{DMS}(\lambda)$) and spectral slopes for DMS photolysis from one ocean region to another with contrasting water types may introduce large uncertainties. Here, we showed that $AQY_{DMS}(330)$ can vary by a factor of three (or more) introducing potential biases on the order of 300%. $AQY_{DMS}(\lambda)$ measurements made in contrasting oceanic environments and in different seasons are needed to further evaluate the extent and functional dependencies of DMS photolysis variability. Additionally, measurements of inherent optical properties of the ocean in the ultraviolet spectral region (280–400 nm) would further reduce the uncertainty in models of DMS photolysis. Investigations focusing on isolating the precursor(s) and mechanism(s) of DMS photolysis will also aid in understanding the variability of DMS photolysis on all spatiotemporal scales.

Acknowledgments

We thank Hiroshi Hattori, Hokkaido Tokai University, for providing the HPLC chlorophyll data, JAMSTEC for providing the nitrate and wind speed data and the captain and crew of the JAMSTEC R/V *Mirai* on Leg 2 MR01-K04 for their assistance in collecting the samples. This work was partly supported by NSF (OPP-0230499, DJK). Any opinions, findings, and conclusions or recommendations expressed in this paper are those of the authors and do not necessarily reflect the views of the NSF.

References

Barnard, W.R., Andreae, M.O., Iverson, R.L., 1984. Dimethylsulfide and *Phaeocystis poucheti* in the southeastern Bering Sea. Continental Shelf Research 3 (2), 103–113.

Bates, T.S., Cline, J.D., Gammon, R.H., Kelly-Hansen, S.R., 1987. Regional and seasonal variations in the flux of oceanic dimethylsulfide to the atmosphere. Journal of Geophysical Research 92 (C3), 2930–2938.

Bates, T.S., Kiene, R.P., Wolfe, G.V., Matrai, P.A., Chavez, F.P., Buck, K.R., Blomquist, B.W., Cuhel, R.L., 1994. The cycling of sulfur in surface seawater of the northeast Pacific. Journal of Geophysical Research 99 (C4), 7835–7843.

Bouillon, R.-C., Miller, W.L., 2004. Determination of apparent quantum yield spectra of DMS photodegradation in an in situ iron-induced Northeast Pacific Ocean bloom. Geophysical Research Letters 31, L06310.

Brimblecombe, P., Shooter, D., 1986. Photo-oxidation of dimethylsulphide in aqueous solution. Marine Chemistry 19, 343–353.

Brugger, A., Slezak, D., Obernosterer, I., Herndl, G.J., 1998. Photolysis of dimethylsulfide in the northern Adriatic Sea: dependence on substrate concentration, irradiance and DOC concentration. Marine Chemistry 59, 321–331.

Coachman, L.K., 1986. Circulation, water masses and fluxes on the southeastern Bering Sea shelf. Continental Shelf Research 5, 23–108.

Gjerstad, K.I., Stamnes, J.J., Hamre, B., Lotsberg, J.K., Yan, B., Stamnes, K., 2003. Monte Carlo and discrete-ordinate simulations of irradiances in the coupled atmosphere-ocean system. Applied Optics 42, 2609–2622.

Gordon, H.R., Morel, A., 1983. Remote assessment of ocean color for interpretation of satellite visible imagery, a review. Lecture Notes on Coastal and Estuarine Studies, vol.4, Springer, New York

Green, S.A., Blough, N.V., 1994. Optical absorption and fluorescence properties of chromophoric dissolved organic matter in natural water. Limnology and Oceanography 39 (8), 1903–1916.

Hatton, A.D., 2002. Influence of photochemistry on the marine biogeochemical cycle of dimethylsulphide in the northern North Sea. Deep-Sea Research 49, 3039–3052.

Hill, R.W., White, B.A., Cottrell, M.T., Dacey, J.W.H., 1998. Virus-mediated total release of dimethylsulfoniopropionate from marine phytoplankton: a potential climate process. Aquatic Microbial Ecology 14, 1–6.

Hunt, G.L., Stabeno, P., Walters, G., Sinclair, E., Brodeur, R.D., Napp, J.M., Bond, N.A., 2002. Climate change and control of the southeastern Bering Sea pelagic ecosystem. Deep-Sea Research II 49, 5821–5853.

Huot, Y., Jeffrey, W.H., Davis, R.F., Cullen, J.J., 2000. Damage to DNA in bacterioplankton: a model of damage by ultraviolet radiation and its repair as influenced by vertical mixing. Photochemistry and Photobiology 72 (1), 62–74.

JAMSTEC Preliminary Cruise Report, 2001. R/V *Mirai* Cruise MR01-K04 (Leg 2). WWW Page, http://www.jamstec.go.jp/mirai/2001/data_2001.

Jankowski, J.J., Kieber, D.J., Mopper, K., 1999. Nitrate and nitrite ultraviolet actinometers. Photochemistry and Photobiology 70, 319–328.

Jankowski, J.J., Kieber, D.J., Mopper, K., Neale, P.J., 2000. Development and intercalibration of ultraviolet solar actinometers. Photochemistry and Photobiology 71, 431–440.

Jin, Z., Stamnes, K., 1994. Radiative transfer in nonuniformly refracting media such as the atmosphere/ocean system. Applied Optics 33, 431–442.

Keller, M.D., Bellows, W.K., Guillard, R.R.L., 1989a. Dimethyl sulfide production in marine phytoplankton. In: Saltzman, E.S., Cooper, W.J. (Eds.), Biogenic Sulfur in the Environment. ACS Symposium Series No. 393. American Chemical Society, Washington, DC, pp. 167–182.

Keller, M.D., Bellows, W.K., Guillard, R.R.L., 1989b. Dimethylsulfide production in marine phytoplankton: an additional impact of unusual blooms. In: Cosper, E.M., Bricelj, V.M., Carpenter, E.J. (Eds.), Novel Phytoplankton Blooms. Springer, Berlin, pp. 101–115.

Kieber, D.J., Jiao, J., 1995. Photochemistry of dimethyl sulfide in seawater. Prepr. Amer. Chem. Soc., Div. Environ. Chem. 35, 523–525.

Kieber, D.J., Jiao, J., Kiene, R.P., Bates, T.S., 1996. Impact of dimethylsulfide photochemistry on methyl sulfur cycling in the equatorial Pacific Ocean. Journal of Geophysical Research 101 (C2), 3715–3722.

Kieber, D.J., Yocis, B.H., Mopper, K., 1997. Free-floating drifter for photochemical studies in the water column. Limnology and Oceanography 42, 1829–1833.

Kiene, R.P., Bates, T.S., 1990. Biological removal of dimethyl sulphide from seawater. Nature 345, 702–704.

Kiene, R.P., Service, S.K., 1991. Decomposition of dissolved DMSP and DMS in estuarine waters: Dependence on temperature and substrate concentration. Marine Ecological Progress Series 76, 1–11.

Levasseur, M., Gosselin, M., Michaud, S., 1994. A new source of dimethylsulfide (DMS) for the arctic atmosphere: ice diatoms. Marine Biology 121, 381–387.

Matrai, P.A., Vernet, M., 1997. Dynamics of the vernal bloom in the marginal ice zone of the Barents Sea: Dimethyl sulfide and dimethylsulfoniopropionate budgets. Journal of Geophysical Research 102 (C10), 22965–22979.

Matrai, P.A., Vernet, M., Hood, R., Jennings, A., Brody, E., Saemundsdóttir, S., 1995. Light-dependence of carbon and sulfur production by polar clones of the genus *Phaeocystis*. Marine Biology 124, 157–167.

Miller, G.W., 2000. Wavelength and temperature dependent quantum yields for photochemical formation of hydrogen peroxide in seawater. M.S. thesis, State Univ. of New York, College of Environmental Science and Forestry.

Miller, W.L., Moran, M.A., Sheldon, W.M., Zepp, R.G., Opsahl, S., 2002. Determination of apparent quantum yield spectra for the formation of biologically labile photoproducts. Limnology and Oceanography 47 (2), 343–352.

Morel, A., 1974. Optical properties of pure water and pure seawater. In: Jerlov, N.G., Nielsen, E.S. (Eds.), Optical Aspects in Oceanography. Academic Press, New York, pp. 1–24.

Morel, A., 1980. In water and remote measurements of ocean color. Boundary-Layer Meteorology 18, 177–201.

Morel, A., Maritorena, S., 2001. Bio-optical properties of oceanic waters: A reappraisal. Journal of Geophysical Research 106 (C4), 7163–7180.

National Climate Data Center, 2002. Local Climatological Data Annual Summary with Comparative Data, St. Paul Island, Alaska: Normals, Means and Extremes, Asheville, NC.

Neale, P.J., Kieber, D.J., 2000. Assessing biological and chemical effects of UV in the marine environment: Spectral weighting functions. In: Hester, R.E., Harrison, R.M. (Eds.), Environmental Science and Technology No. 14, Causes and Environmental Implications of Increased UV-B

Radiation. Royal Society of Chemistry, Cambridge, UK, pp. 61–83.

Nelson, N.B., Siegel, D.A., 2002. Chromophoric DOM in the open ocean. In: Hansell, D.A., Carlson, C.A. (Eds.), Biogeochemistry of Marine Dissolved Organic Matter. Elsevier Science, USA, pp. 547–578.

Nguyen, B.C., Belviso, S., Mihalopoulos, N., Gostan, J., Nival, P., 1988. Dimethyl sulfide production during natural phytoplankton blooms. Marine Chemistry 24, 133–141.

Pope, R.M., Fry, E.S., 1997. Absorption spectrum ((380–700 nm) of pure water. II. Integrating cavity measurements. Applied Optics 36 (33), 8710–8723.

Preiswerk, D., Najjar, R.G., 2000. A global, open-ocean model of carbonyl sulfide and its air-sea flux. Global Biogeochemical Cycles 14 (2), 585–598.

Saltzman, E.S., King, D.B., Holmen, K., Leck, C., 1993. Experimental determination of the diffusion coefficient of dimethylsulfide in water. Journal of Geophysical Research 98 (C9), 16481–16486.

Sasaki, H., Saitoh, S., Kishino, M., 2001. Bio-optical properties of seawater in the western subarctic gyre and Alaskan gyre in the subarctic North Pacific and the southern Bering Sea during the Summer of 1997. Journal of Oceanography 57, 275–284.

Slezak, D., Brugger, A., Herndl, G.J., 2001. Impact of solar radiation on the biological removal of dimethylsulfoniopropionate and dimethylsulfide in marine surface waters. Aquatic Microbial Ecology 25, 87–97.

Smith, R.C., Baker, K.S., 1981. Optical properties of the clearest natural waters (200–800 nm). Applied Optics 20, 177–184.

SooHoo, J.B., Palmisano, A.C., Kottmeier, S.T., Lizotte, M.P., SooHoo, S.L., Sullivan, C.W., 1987. Spectral light absorbance and quantum yield of photosynthesis in sea ice microalgae and bloom of *Phaeocystis pouchetti* from McMurdo Sound, Antarctica. Journal of Marine Ecological Progress Series 39, 175–189.

Sunda, W., Kieber, D.J., Kiene, R.P., Huntsman, S., 2002. An antioxidant function for DMSP and DMS in marine algae. Nature 418, 317–320.

Thomas, G.E., Stamnes, K., 1999. Radiative Transfer in the Atmosphere and Ocean. Cambridge University Press, UK.

Toole, D.A., Kieber, D.J., Kiene, R.P., Siegel, D.A., Nelson, N.B., 2003. Photolysis and the dimethylsulfide (DMS) summer paradox in the Sargasso Sea. Limnology and Oceanography 48 (3), 1088–1100.

Toole, D.A., Kieber, D.J., Kiene, R.P., White, E.M., Bisgrove, J., del Valle, D.A., Slezak, D., 2004. High dimethylsulfide photolysis rates in nitrate-rich Antarctic Waters. Geophysical Research Letters 31, L11307.

Uzuka, N., Guo, L., Tanaka, T., 2001. Research topics on R/V *Mirai* Cruise MR01-K04 (Leg 2) carried out by Observational Frontier Research Program, In: JAMSTEC Preliminary Cruise Report. WWW Page, http://www.jamstec.go.jp/mirai/2001/data_2001, pp. 93–94.

Wakeham, S.G., Dacey, J.W.H., 1989. Biogeochemical cycling of dimethyl sulfide in marine environments. In: Saltzman, E.S., Cooper, W.J. (Eds.), Biogenic Sulfur in the Environment. American Chemical Society, Washington, DC, pp. 152–166.

Wanninkhof, R., McGillis, W.R., 1999. A cubic relationship between air-sea CO_2 exchange and wind speed. Geophysical Research Letters 26 (13), 1889–1892.

Whitledge, T.E., Luchin, V.A., 1999. Summary of chemical distributions and dynamics in the Bering Sea. In: Loughlin, T.R., Ohtani, K. (Eds.), Dynamics of the Bering Sea: A Summary of Physical, Chemical, and Biological Characteristics. University of Alaska Sea Grant, Fairbanks, AK, pp. 217–249.

Wolfe, G.V., Steinke, M., 1996. Grazing-activated production of dimethyl sulfide (DMS) by two clones of *Emiliania huxleyi*. Limnology and Oceanography 41 (6), 1151–1160.